Original Paper

Audiology & Neurotology

Audiol Neurotol 2013;18:143–151
DOI: 10.1159/000346344

Received: June 23, 2012
Accepted after revision: December 6, 2012
Published online: January 31, 2013

Effect of Vestibular Dysfunction on the Development of Gross Motor Function in Children with Profound Hearing Loss

Aki Inoue Shinichi Iwasaki Munetaka Ushio Yasuhiro Chihara
Chisato Fujimoto Naoya Egami Tatsuya Yamasoba

Department of Otolaryngology, Faculty of Medicine, University of Tokyo, Tokyo, Japan

Key Words
Vestibular evoked myogenic potential · Caloric test · Rotational test · Gross motor development

Abstract
Objective: To evaluate the function of the superior and inferior vestibular nerve systems in children with profound sensorineural hearing loss, and to assess the influence of dysfunction of each vestibular nerve system on the development of gross motor function. ***Study Design:*** Retrospective study. ***Setting:*** A tertiary referral center. ***Methods:*** Eighty-nine children (age range: 20–97 months) with profound sensorineural hearing loss who were due to undergo cochlear implant surgery were recruited. Function of the superior vestibular nerve system was evaluated by the damped rotation test and the caloric test, whereas functions of the inferior vestibular nerve systems were evaluated by the vestibular evoked myogenic potential (VEMP) test. Gross motor development was assessed using the age of acquisition of head control and independent walking. ***Results:*** Among the children able to complete the vestibular function tests, abnormalities were found in 20% (16 of 84 children) in the damped rotation test, 41% (31 of 75 children) in the caloric test and 42% (26 of 62 children) in the VEMP test. Children who showed abnormal responses in the vestibular function tests showed significantly delayed acquisition of head control ($p < 0.05$) and independent walking ($p < 0.05$) in comparison with children with normal responses. The children who showed abnormal responses in all 3 vestibular tests showed the greatest delay in acquisition of gross motor function in comparison with the other groups. ***Conclusions:*** Children with profound hearing loss tend to have dysfunction in the superior as well as the inferior vestibular nerve systems. Both the superior and inferior vestibular nerve systems are important for the development of gross motor function in children.

Introduction

The development of balance and gross motor functions such as head control and independent walking are intimately related and dependent on inputs from the vestibular, visual, proprioceptive and motor systems [Kaga, 1999; Suarez et al., 2007]. During the early stages of development, children primarily depend on the visual system to maintain balance. As they grow older, they progressively begin to use somatosensory and vestibular information until these systems reach full maturity around the age of 10 years [Kaga, 1999; Wallacott et al., 2004;

KARGER
E-Mail karger@karger.com
www.karger.com/aud

1420–3030/13/0183–0143$38.00/0

Shinichi Iwasaki, MD
Department of Otolaryngology, Faculty of Medicine
University of Tokyo, 7-3-1 Hongo
Bunkyo-ku, Tokyo 113-8655 (Japan)
E-Mail iwashin-tky@umin.ac.jp

Suarez et al., 2007]. Since vestibular function plays an important role in the development of balance and locomotion, impairment of the vestibulospinal system in infancy may lead to delayed achievement of gross motor milestones [Eviatar et al., 1979; Kaga, 1999; Kaga et al., 2008].

A close relationship exists between the cochlea and the peripheral vestibular end organs with respect to embryology, physiology and anatomy [Jin et al., 2006; Cushing et al., 2008a], hence they may be similarly affected by embryological factors, or by viral or bacterial infections. Therefore, children with profound sensorineural hearing loss may also exhibit peripheral vestibular impairments [Shinjo et al., 2007; Cushing et al., 2008a; Kaga et al., 2008; Jacot et al., 2009]. It has been reported that children with profound hearing loss tend to display balance dysfunction and delayed acquisition of gross motor skills, such as head control, sitting and walking, compared with children with normal hearing [Potter and Silverman, 1984; Butterfield, 1986; Crowe and Horak, 1988; Suarez et al., 2007; Cushing et al., 2008a]. The incidence of vestibular dysfunction in children with profound hearing loss has been reported to be between 31 and 75% [Diepeveen and Jensen, 1968; Jin et al., 2006; Cushing et al., 2008a; Zagólski, 2008].

Several previous studies have investigated the relationship between vestibular function and gross motor development in children with profound hearing loss [Kaga et al., 1981; Potter and Silverman, 1984; Crowe and Horak, 1988; Suarez et al., 2007; Cushing et al., 2008a]. Kaga et al. [1981] showed that the age of acquiring head control and independent walking in children with vestibular dysfunction was significantly delayed compared with normal controls [Kaga et al., 1981]. Rine et al. [2000] reported delayed gross motor development in children with vestibular dysfunction. In these studies, vestibular function in infants and children was evaluated using the rotational test and/or the caloric test, which reflect function in the lateral semicircular canal and superior vestibular nerves [Kaga, 1999; Suarez et al., 2007; Cushing et al., 2008a]. Vestibular evoked myogenic potentials (VEMPs) in response to air-conducted sound have recently been used to evaluate vestibular function [Colebatch and Halmagyi, 1992; Murofushi et al., 1996, 1998; Welgampola and Colebatch, 2005]. Physiological and clinical studies have suggested that VEMPs are generated by activation of the saccule and the inferior vestibular nerves [McCue and Guinan, 1994; Murofushi et al., 1995, 1996]. Combined use of VEMP and rotational and/or caloric tests has enabled examination of the inferior and superior vestibular nerve systems separately [Murofushi et al., 1996, 1998; Iwasaki et al., 2005]. Although VEMPs have been studied mainly in adults, it has been shown that the VEMP can be recorded from infants and children in almost the same way as adults [Kelsch et al., 2006].

In the present study, we assessed vestibular function in children with profound hearing loss, before they underwent cochlear implantation, using VEMPs as well as caloric and rotational testing, and compared the results with the development of gross motor function. The purposes of the present study were to evaluate the function of the superior and inferior vestibular nerve systems in children with profound hearing loss, and to investigate the effect of each vestibular nerve system on the development of gross motor function.

Methods

We enrolled 101 consecutive new children (20–97 months old) who presented at the University of Tokyo Hospital between January 2003 and June 2010 with profound hearing loss and who subsequently underwent cochlear implant surgery. We excluded 11 children with acquired hearing loss (4 due to meningitis, 2 due to severe neonatal infections, and 5 who had passed the newborn hearing screening test). We also excluded 1 child with extremely low birth weight. We did not exclude 8 children with cytomegalovirus (CMV) infection or 2 with Waardenburg syndrome because they did not show any neurological abnormalities except for hearing loss. As a result, 89 children (45 male, 44 female; age range 20–97 months, mean age 40 months) were included. The data of individual children are listed in the online supplementary table 1 (see www.karger.com/doi/10.1159/000346344 for all online suppl. material). All these patients underwent high-resolution computed tomography of the temporal bone and magnetic resonance imaging of the brain. Screening for the connexin 26 *(GJB2)* mutation in the peripheral blood and screening for CMV DNA in the umbilical cord blood were performed in 31 and 28 patients, respectively. The etiologies of hearing loss in the 89 children are listed in table 1. Classification of the inner ear malformation [Sennaroglu and Saatci, 2002] in 19 patients is listed in the online supplementary table 2.

This study was approved by the ethics committee in the Faculty of Medicine at the University of Tokyo and was conducted according to the tenets of the Declaration of Helsinki. Written informed consent was obtained from the parents of each participant.

Evaluation of the Etiologies of Hearing Loss

High-resolution computed tomographic scans (slice thickness 1.0 mm), screening for CMV DNA in the umbilical cord blood, and screening for the *GJB2* mutation were performed. High-resolution computed tomographic scans were checked by both otolaryngologists and radiologists. Both homozygous and heterozygous mutations of *GJB2* were classified as positive. There was no patient selection protocol with regard to the performance of these tests, which may cause a bias in the etiology results. A family history of significant perinatal problems was checked by having parents complete questionnaires (open-ended questions). These procedures were approved by the local ethics committee.

Table 1. Etiologies of hearing loss in 89 children

	Number %	Mean age at evaluation, months
Inner ear malformation	19 (21%)	43 (25–87)
GJB2 mutation	13 (15%)	27 (20–33)
Congenital CMV infection	8 (9%)	38 (24–63)
Waardenburg syndrome	2 (2%)	51 (27–75)
Unknown	47 (54%)	42 (24–97)
Total	89 (100%)	40 (20–97)

Age ranges are indicated in parentheses.

Vestibular Function Tests

Damped Rotation Test

The children were held upright on their mother's knees on a rotational chair with their heads bending down 30°. The rotational chair was accelerated to a maximum rotational velocity of 200°/s with a maximum acceleration of 300°/s^2 and then decayed to 0°/s by a deceleration of −4°/s^2. The test was conducted twice in both clockwise and counterclockwise directions. Eye movements were recorded by electronystagmography. Since calibration for accurate velocity measurements could not be performed in most children, we calculated the number of beats of per-rotatory nystagmus. The number of beats was measured and compared with age-matched controls according to the results of the damped rotation test in normal children reported by Kaga et al. [1981] for children up to 6 years old. If the number of per-rotatory nystagmus beats was more than 2 standard deviations smaller than the average value at each age, as reported by Kaga et al. [1981], it was considered abnormal. For children older than 6 years, the normal limit of the number of per-rotatory nystagmus beats was set as 23. This value is based on the number of per-rotatory nystagmus beats in 15 normal children between the ages of 7 and 9 years (31 ± 3.9 beats) recorded in this laboratory.

Caloric Test

The caloric test was performed using 4°C ice water. Horizontal and vertical eye movements were recorded using electronystagmography. We measured the duration of induced nystagmus and compared it with age-matched controls since calibration of eye movements was difficult in most children. The duration of induced nystagmus in 112 normal control children was 94.7 ± 20.7 s for the age range 13–24 months, 103.8 ± 28.4 s for 25–36 months, 109.2 ± 28.4 s for 37–48 months, 98.1 ± 20.3 s for 49–60 months, 105 ± 28.4 for 61–72 months, and 123.3 ± 35.1 s for >72 months. If the duration of induced nystagmus was more than 2 standard deviations smaller than the average value at each age, it was considered abnormal. Therefore, normal limits were set as 53.3 s for 13–24 months, 54.3 s for 25–36 months, 52.4 s for 37–48 months, 57.4 s for 49–60 months, 48.1 s for 61–72 months and 35.1 s for >72 months.

Vestibular Evoked Myogenic Potentials

Each subject was placed in the supine position. The active electrode was placed over the upper half of the sternocleidomastoid muscle (SCM), the reference electrode on the upper sternum and the ground electrode on the midline of the forehead. Subjects were instructed to raise their heads off the pillow to activate the SCM. In children who could not follow this instruction, the examiner helped them to raise their body with their head hanging down to induce contraction of the SCM. Electromyographic activity in the SCMs was monitored to confirm sufficient normal muscle activity (>150 μV). Sound stimuli of 500-Hz tone bursts (95 dB nHL) were presented to each ear through calibrated headphones (DR-531, Elega Acoustic Co. Ltd., Tokyo, Japan). Electromyographic signals from the SCM on the stimulated side were amplified using Neuropack Sigma (Nihon Koden, Tokyo, Japan). The stimulation rate was 5 Hz, the band-pass filter intensity was 20–2000 Hz, and the analysis time was 50 ms. VEMPs in response to 50 stimuli were averaged twice. VEMPs were considered to be present when there was a reproducible short-latency biphasic wave (p13–n23) [Sheykholeslami et al., 2005; Kelsch et al., 2006]. We calculated the asymmetry ratio for the amplitude of VEMPs (VEMP AR) with the following formula using the peak-to-peak amplitude of p13–n23 (μV) on the right side *(Ar)* and that on the left side *(Al)*:

$$\text{VEMP AR (\%)} = 100 \cdot |(Ar - Al)/(Ar + Al)|.$$

VEMP AR (%) <33.3 was considered to indicate a significant asymmetry [Jin et al., 2006; Shinjo et al., 2007].

Gross Motor Development

To assess gross motor development, we interviewed parents about the age at which the children started to acquire head control and to walk by themselves. We also checked the ages given against the relevant data recorded in the Maternity Health Record Book provided by the Japanese government.

If the age of acquiring head control was >5 months and the age of independent walking was >18 months, the development of the gross motor function was considered to be delayed according to the modified version of DENVER II for Japanese children published by the Japanese Society of Child Health (Nihon Shoni Iji Shuppansha, Tokyo, Japan).

Statistics

For comparison of two groups, the Mann-Whitney U test was used. For comparing multiple groups, the nonparametric Kruskal-Wallis test was used. Variables that showed a significant difference in this test were then compared in pairs using the nonparametric Steel-Dwass multiple-comparison method. Values were expressed as means ± SD. A p value <0.05 was considered significant.

Results

Vestibular Function in Children with Profound Hearing Loss

A summary of the results of the damped rotation test, caloric test and VEMPs in the children with profound hearing loss is shown in table 2. Since these vestibular tests need a certain amount of cooperation, they could not be completed in some children. Among the 89 children recruited, 51 were able to complete all 3 vestibular tests

Table 2. Results of vestibular function testing

	Normal	Unilateral dysfunction	Bilateral dysfunction	Total
Inner ear malformation				
Rotation test	9 (50%)	0 (0%)	9 (50%)	18 (100%)
Caloric test	4 (27%)	4 (27%)	7 (47%)	15 (100%)
VEMP	6 (40%)	2 (13%)	7 (47%)	15 (100%)
GJB2 mutation				
Rotation test	13 (100%)	0 (0%)	0 (0%)	13 (100%)
Caloric test	13 (100%)	0 (0%)	0 (0%)	13 (100%)
VEMP	10 (83%)	0 (0%)	2 (17%)	12 (100%)
Congenital CMV infection				
Rotation test	3 (60%)	1 (20%)	1 (20%)	5 (100%)
Caloric test	4 (67%)	1 (17%)	1 (17%)	6 (100%)
VEMP	2 (33%)	1 (17%)	3 (50%)	6 (100%)
Others				
Rotation test	42 (88%)	0 (0%)	6 (13%)	48 (100%)
Caloric test	23 (56%)	8 (20%)	10 (24%)	41 (100%)
VEMP	18 (62%)	2 (7%)	9 (31%)	29 (100%)
All children				
Rotation test	67 (80%)	1 (1%)	16 (19%)	84 (100%)
Caloric test	44 (59%)	13 (17%)	18 (24%)	75 (100%)
VEMP	36 (58%)	5 (8%)	21 (34%)	62 (100%)

Table 3. Relationship between superior and inferior vestibular function tests

	Rotation test/caloric test			Total
	normal	asymmetry	bilateral dysfunction	
VEMP				
Normal	26	7	1	36
Asymmetry	1	3	1	5
Bilateral dysfunction	9	0	11	20
Total	36	10	15	61

whereas the other 38 children were only able to complete 1 or 2 of the tests.

The damped rotation test was completed in 84 of the 89 children (94%). Among these 84 children, 16 (19%) showed reduced or absent per-rotatory nystagmus on both clockwise and counterclockwise rotations, whereas 67 children (80%) showed normal responses during rotation in both directions. One child (1%) showed reduced per-rotatory nystagmus in the clockwise rotations only (patient No. 36 in the online suppl. table 1).

Caloric testing was completed in 75 of the 89 children (84%). Among them, 18 children (24%) showed reduced or absent nystagmus induced in both ears, whereas 44 children (59%) showed normal responses in both ears. Thirteen children (17%) showed abnormal responses in one ear only.

VEMP testing was completed in 62 of the 89 children (70%). Among them, 21 children (34%) showed no responses on either side whereas 36 children (58%) showed normal responses on both sides. Five children (8%) showed responses on one side only.

Most children with the *GJB2* mutation showed normal responses bilaterally in the damped rotation test, caloric test and VEMP test. On the other hand, more than half of the children with inner ear malformations and congenital CMV infection showed abnormal responses in these 3 vestibular function tests (table 2).

The relationship between the results of the damped rotation test, caloric test and VEMP test are shown in table 3. Since both the damped rotation and caloric tests reflect the function of the superior vestibular nerve system, we combined the results of these two tests. If cases showed abnormal responses in either of these two tests, we classified them as having abnormal superior vestibular function. Cases which showed abnormal VEMP responses were classified as having abnormal inferior vestibular function. Among the 61 children who were able to complete all 3 vestibular tests, 26 (43%) showed normal responses in both the superior and inferior vestibular function tests whereas 15 children (25%) showed abnormal responses in both of these tests. Ten children (16%) showed abnormalities in the superior vestibular function tests while sparing inferior vestibular function. On the other hand, 10 children (16%) showed abnormalities in the inferior vestibular dysfunction tests while sparing superior vestibular nerve function.

Gross Motor Development in Children with Profound Hearing Loss

The distribution of ages at which children with profound hearing loss started acquiring head control and independent walking are shown in figure 1 and table 4. We were unable to obtain information regarding the age of acquisition of head control in 10 children, and the age of independent walking in 13 children.

The age at which the children acquired head control was delayed to later than 5 months of age in 24 (30%) of 79 children. The age at which children began to walk independently was delayed to later than 18 months of age in 20 (26%) of 76 children.

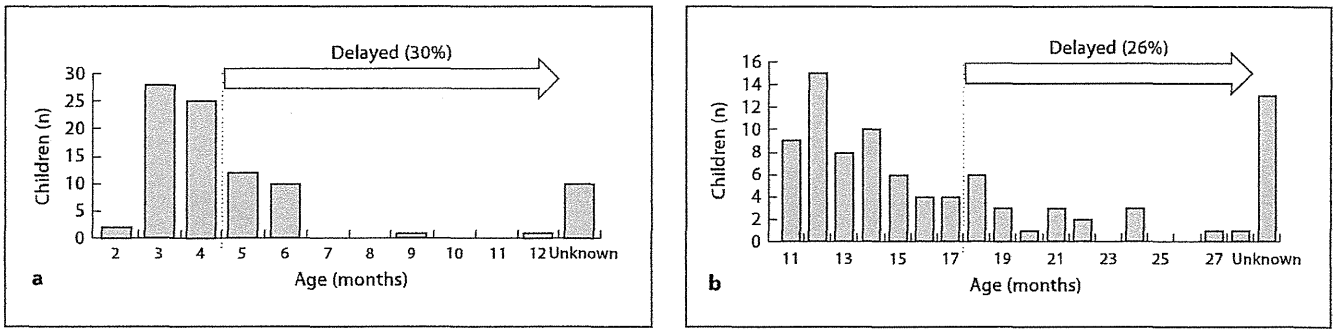

Fig. 1. Distribution of the age of acquiring head control and independent walking in children with profound hearing loss. **a** Distribution of the age of acquiring head control. Ages greater than 5 months were considered to be delayed. **b** Distribution of the age of independent walking. Ages greater than 18 months were considered to be delayed.

Table 4. Age of acquiring head control and independent walking

	Head control			Independent walking			Total
	normal	delayed	unknown	normal	delayed	unknown	
Inner ear malformation	8 (42%)	8 (42%)	3 (16%)	8 (42%)	7 (37%)	4 (21%)	19 (100%)
GJB2 mutation	11 (85%)	1 (8%)	1 (8%)	13 (100%)	0	0	13 (100%)
Congenital CMV infection	6 (50%)	1 (13%)	1 (13%)	4 (50%)	2 (25%)	2 (25%)	8 (100%)
Others	30 (4%)	14 (29%)	5 (10%)	31 (63%)	11 (22%)	7 (14%)	49 (100%)
All children	55 (62%)	24 (27%)	10 (11%)	56 (33%)	20 (22%)	13 (15%)	89 (100%)

In most children with the *GJB2* mutation, the age of acquiring head control and independent walking was within normal limits (11 of 12 children with available information for head control; all children with available information for independent walking; table 4). On the other hand, approximately half of the children with inner ear malformations showed delayed head control (8 of 16 children) and delayed independent walking (7 of 15 children). In children with CMV infection, the age of independent walking was delayed in one third (2 of 6 children) whereas the age of acquiring head control was delayed in one seventh of them (1 of the 7 children).

Vestibular Function and the Development of Gross Motor Function

To estimate the effect of vestibular dysfunction on the development of gross motor function, we compared the age of acquiring head control and independent walking with the results of each of the vestibular function tests (table 5). The age of acquiring both head control and independent walking was significantly delayed in children who showed abnormal responses bilaterally in comparison with those who showed normal responses bilaterally ($p < 0.05$ in the rotation test, caloric test and VEMP test for both head control and independent walking). On the other hand, there were no significant differences in the age of acquiring head control and independent walking between the children who showed asymmetric responses and those with normal responses in the caloric and VEMP testing ($p > 0.05$ for both tests).

To clarify the effect of dysfunction of the superior and inferior vestibular nerve systems on the development of gross motor function, we classified the children according to the involvement of the superior and the inferior vestibular nerve systems into the following 4 groups: (1) normal group, i.e. children who showed normal responses bilaterally in both the superior vestibular function tests (caloric testing and damped rotation test) and the inferior vestibular function test (VEMPs) (n = 26); (2) superior dysfunction group, i.e. those with abnormal re-

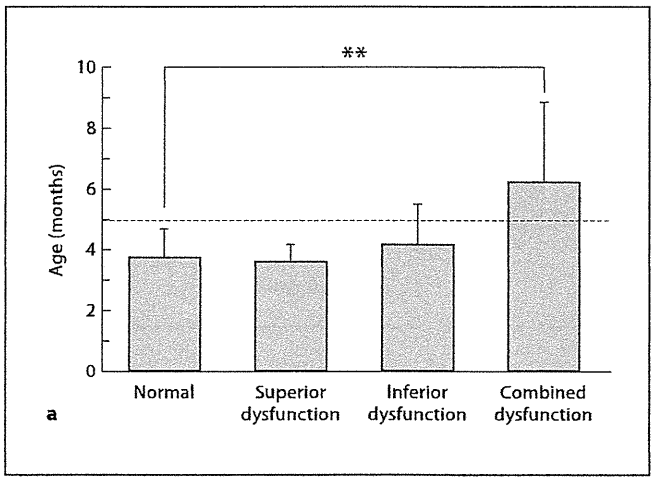

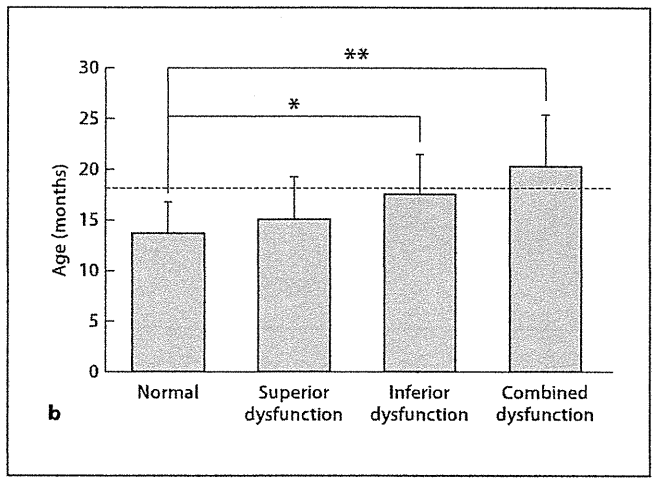

Fig. 2. Comparison of the age of acquiring head control and independent walking in children with profound hearing loss classified according to the involvement of the superior and inferior vestibular nerve systems. * $p < 0.05$, ** $p < 0.01$. **a** The age of acquiring head control in children with normal vestibular function, those with involvement of the superior vestibular nerve system sparing the inferior vestibular nerve system (superior dysfunction), those with involvement of the inferior vestibular nerve system sparing the superior vestibular nerve system (inferior dysfunction) and those with involvement of both the superior and inferior vestibular nerve systems (combined dysfunction). **b** The age of independent walking in the normal, superior, inferior and combined dysfunction groups.

Table 5. Age (months) of gross motor development in relation to vestibular function test results

	Normal	Asymmetry	Bilateral dysfunction
Head control			
Rotation test	3.8±1.1 (59)	3 (1)	5.6±2.3 (14)
Caloric test	3.7±1.0 (37)	4.0±1.0 (12)	5.2±2.2 (17)
VEMP	3.7±0.8 (31)	4.8±1.1 (5)	5.3±2.2 (19)
Independent walking			
Rotation test	14.6±3.5 (59)	14 (1)	19.1±4.8 (12)
Caloric test	14.5±3.8 (39)	14.0±2.1 (12)	18.4±5.0 (15)
VEMP	13.7±2.7 (29)	15.8±4.6 (4)	18.8±4.7 (17)

Data are shown as means ± SD; numbers of children are indicated in parentheses.

sponses bilaterally in either of the superior vestibular function tests in the presence of normal VEMP responses bilaterally (n = 9); (3) inferior dysfunction group, i.e. those with abnormal VEMP responses bilaterally in the presence of normal superior vestibular function tests (n = 3), and (4) combined dysfunction group, i.e. those with abnormal responses bilaterally in both the superior and inferior vestibular function tests (n = 11). Ten patients who showed unilateral vestibular dysfunction in either the damped rotation test or the caloric test (patients No. 12, 14, 15, 38, 50, 51, 57, 62, 64 and 69 in the online suppl. table 1) and 5 patients who showed abnormal VEMP responses on one side (patients No. 12, 14, 38, 77 and 83) were excluded from this analysis. Among them, 2 children (patients No. 14 and 38) showed dysfunction on the same sides in both caloric and VEMP tests, whereas the other children showed dysfunction on different sides in these tests. The age of acquiring head control was significantly delayed in the combined dysfunction group in comparison with the normal group ($p < 0.01$), whereas there were no significant differences among the normal group, the superior dysfunction group and the inferior dysfunction group ($p > 0.1$; fig. 2a). The age of independent walking was significantly delayed in the combined dysfunction group and in the inferior dysfunction group compared with the normal group ($p < 0.01$ and $p < 0.05$, respectively), whereas there were no significant differences between the normal group and the superior dysfunction group ($p > 0.8$) or between the inferior dysfunction group and the combined dysfunction group ($p > 0.5$; fig. 2b).

Discussion

In the present study, we have shown that approximately 40% of children with profound hearing loss have dysfunction of the superior vestibular nerve system, approximately 40% have dysfunction of the inferior vestibular nerve system, and approximately 20% have dysfunction of both vestibular nerve systems. Acquisition of head control and independent walking in children with bilateral vestibular dysfunction was significantly delayed in comparison with those with normal vestibular function.

In previous studies, vestibular function in infants and children has been evaluated by rotation and caloric tests, which reflect the function of the lateral semicircular canals and superior vestibular nerve [Diepeveen and Jensen, 1968; Kaga et al., 1981; Kaga, 1999; Buchmann et al., 2004; Shinjo et al., 2006; Jacot et al., 2009]. Kaga et al. [1981] examined vestibular function using the damped rotation test in 22 children with congenital deafness and found hypoactivity of the vestibulo-ocular reflexes in 12 children (55%). Shinjo et al. [2007] assessed vestibular function in 20 children with severe hearing loss using the damped rotation and caloric tests, and reported that abnormalities were found in 85% of these children with caloric testing and in 30% with the rotation test. Jacot et al. [2009] examined 224 children with profound hearing loss, using the caloric and rotation tests. They showed that 50% of the children tested have unilateral or bilateral vestibular dysfunction. In the present study, 41% of the children tested showed abnormal caloric responses and 20% showed abnormal responses in the damped rotation test. This prevalence of vestibular dysfunction was lower compared to that of previous studies [Kaga et al., 1981; Shinjo et al., 2007; Jacot et al., 2009]. This discrepancy might be caused by differences between the patient groups since the number of children with the *GJB2* mutation was relatively higher in our study compared to those previous studies [Buchman et al., 2004; Shinjo et al., 2007]. In the present study, most children with the *GJB2* mutation showed normal responses bilaterally in the damped rotation test, caloric test and with VEMPs. This result is consistent with previous reports showing that vestibular function is rarely affected in patients with the *GJB2* mutation [Todt et al., 2005; Tsukada et al., 2010]. On the other hand, more than half of the children with inner ear malformations and congenital CMV infection showed abnormal vestibular function in at least 1 of the 3 kinds of vestibular function tests used in the present study.

VEMPs in response to air-conducted sound have been used to evaluate vestibular function, especially that of the saccule and inferior vestibular afferents [Welgampola and Colebatch, 2005]. Combined use of VEMPs and the caloric test has enabled examination of the superior and inferior vestibular nerve systems separately [Murofushi et al., 1998; Iwasaki et al., 2005]. VEMPs have been extensively studied primarily in adult subjects since VEMPs require neck contraction during recording. However, several recent studies have shown that VEMPs can be recorded from infants and children in almost the same way as adults [Tribukait et al., 2004; Jin et al., 2006; Kelsh et al., 2006; Shinjo et al., 2007]. Tribukait et al. [2004] recorded VEMPs in 39 deaf children between the ages of 15 and 17 years and reported that VEMPs were absent bilaterally in 22% and asymmetric in 19%. Shinjo et al. [2007] recorded VEMPs in 20 children with profound deafness with ages ranging from 2 to 7 years and reported that 20% of patients showed no responses bilaterally and 30% showed asymmetric responses. In the present study, we attempted to record VEMPs from children by helping them to raise their heads during the recording. Furthermore, we used a 95-dB nHL tone burst instead of 90-dB nHL clicks, which were used in the study by Kelsch et al. [2006], as a stimulus for eliciting VEMPs, since it has been shown that tone bursts are superior to clicks in eliciting VEMP responses [Murofushi et al., 1999; Viciana and Lopez-Escamez, 2012]. Of the children tested in this study, with an age range of 2–8 years, 70% were able to generate sufficient neck muscle activity (>150 μV) to successfully complete VEMP testing. Among these children, 8% showed asymmetric VEMP responses and 34% showed no VEMP responses on either side, indicating that approximately 40% of these children with profound hearing loss have dysfunction of the inferior vestibular system on at least one side. This finding is compatible with the finding in previous studies in terms of the percentage of children showing inferior nerve system dysfunction [Tribukait et al., 2004; Shinjo et al., 2007].

In the present study, both the ages of acquiring head control and independent walking were significantly delayed in children with vestibular dysfunction in comparison with those with normal vestibular function. All the children were able to walk independently within 30 months. A few previous studies have shown that gross motor development is delayed in children with bilateral vestibular dysfunction [Kaga et al., 1981; Rine et al., 2000]. Kaga et al. [1981] reported that the age of acquiring head control and independent walking in children with bilateral vestibular dysfunction was significantly delayed

when compared with normal controls. They also reported that all children of preschool age with vestibular dysfunction were able to achieve head control, independent walking and running, suggesting the substitution of vestibular function by other sensory inputs such as visual and somatosensory cues [Kaga et al., 1981; Wallacott et al., 2004]. The development of gross motor function is affected by various factors including the functioning of the visual, vestibular, proprioceptive and motor systems [Kaga, 1999; Wallacott et al., 2004; Suarez et al., 2007]. It has been shown that a substantial proportion of children with profound hearing loss show balance dysfunction, especially when visual and/or somatosensory information is disturbed [Suarez et al., 2007; Cushing et al., 2008b]. Since the relative importance of visual, vestibular and somatosensory inputs to head stabilization and balance control has been shown to change dynamically during preschool ages [Berger et al., 1987; Assaiante and Ambrad, 1992], it is possible that the contribution of visual and somatosensory inputs steadily increases with age in children with vestibular dysfunction. Several studies have shown that children with bilateral vestibular dysfunction show postural instability in conditions with reduced visual and/or somatosensory cues [Enbom et al., 1991; Cushing et al., 2008b].

The contribution of the superior and inferior vestibular nerve systems to the development of gross motor function has not been studied previously. We classified children with profound hearing loss into 4 groups according to the results of 3 vestibular tests (normal function, superior dysfunction, inferior dysfunction, combined dysfunction) and compared the gross motor development among these groups. The age at acquisition of both head control and independent walking in the combined dysfunction group was the latest among the 4 groups, suggesting that the inferior as well as the superior nerve systems play an important role in gross motor development. Furthermore, the age of acquiring independent walking was significantly delayed in the inferior dysfunction group as well as the combined dysfunction group in comparison with the normal group, whereas it was not significantly different between the superior dysfunction group and the normal group. The inferior vestibular nerve system, which has an input to neck and leg muscles, may have a greater influence on the acquisition of independent walking than the superior vestibular nerve system.

In conclusion, we have shown that a substantial proportion of children with profound hearing loss have dysfunction of the inferior as well as the superior vestibular nerve system and that they show delayed acquisition of gross motor function. Since the development of gross motor function varies according to the extent of the involvement of each vestibular nerve system, it is preferable to evaluate both the superior and inferior vestibular function separately in order to form an individualized treatment plan for each child with profound hearing loss.

Acknowledgements

This study was supported by the Ministry of Education, Culture and Technology (22591875).

Disclosure Statement

We have no conflicts of financial interest in this paper.

References

Assaiante C, Amblard B: Peripheral vision and age-related differences in dynamic balance. Hum Mov Sci 1992;11:533–548.

Berger W, Quintern J, Dietz V: Afferent and efferent control of stance and gait: developmental changes in children. Electroencephalogr Clin Neurophysiol 1987;66:244–252.

Buchman CA, Joy J, Hodges A, Telischi FF, Balkany TJ: Vestibular effects of cochlear implantation. Laryngoscope 2004;114:1–22.

Butterfield SA: Gross motor profiles of deaf children. Percept Mot Skills 1986;62:68–70.

Colebatch JG, Halmagyi GM: Vestibular evoked potentials in human neck muscles before and after unilateral vestibular deafferentation. Neurology 1992;42:1635–1636.

Crowe TK, Horak FB: Motor proficiency associated with vestibular deficits in children with hearing impairments. Phys Ther 1988;68:1493–1499.

Cushing SL, Chia R, James AL, Papsin BC, Gordon KA: A test of static and dynamic balance function in children with cochlear implants: the vestibular Olympics. Arch Otolaryngol Head Neck Surg 2008a;134:34–38.

Cushing SL, Papsin BC, Rutka JA, James AL, Gordon KA: Evidence of vestibular and balance dysfunction in children with profound sensorineural hearing loss using cochlear implants. Laryngoscope 2008b;118:1814–1823.

Diepeveen JE, Jensen J: Differential caloric reactions in deaf children. Acta Otolaryngol 1968;65:570–574.

Enbom H, Magnusson M, Pyykko I: Postural compensation in children with congenital or early acquired bilateral vestibular loss. Ann Otol Rhinol Laryngol 1991;100:472–478.

Eviatar L, Miranda S, Eviatar A, Freeman K, Borkowski M: Development of nystagmus in response to vestibular stimulation in infants. Ann Neurol 1979;5:508–514.

Iwasaki S, Takai Y, Ito K, Murofushi T: Abnormal vestibular evoked myogenic potentials in the presence of normal caloric responses. Otol Neurotol 2005;26:1196–1199.

Jacot E, van den Abbeele T, Debre HR, Wiener-Vacher SR: Vestibular impairments pre- and post-cochlear implant in children. Int J Pediatr Otorhinolaryngol 2009;73:209–217.
Jin Y, Nakamura M, Shinjo Y, Kaga K: Vestibular-evoked myogenic potentials in cochlear implant children. Acta Otolaryngol 2006;126:164–169.
Kaga K: Vestibular compensation in infants and children with congenital and acquired vestibular loss in both ears. Int J Pediatr Otorhinolaryngol 1999;49:215–224.
Kaga K, Shinjo Y, Jin Y, Takegoshi H: Vestibular failure in children with congenital deafness. Int J Audiol 2008;47:590–599.
Kaga K, Suzuki JI, Marsh RR, Tanaka Y: Influence of labyrinthine hypoactivity on gross motor development of infants. Ann NY Acad Sci 1981;374:412–420.
Kelsch TA, Schaefer LA, Esquivel CR: Vestibular evoked myogenic potentials in young children: test parameters and normative data. Laryngoscope 2006;116:895–900.
McCue MP, Guinan JJ: Acoustically responsive fibers in the vestibular nerve of the cat. J Neurosci 1994;14:6058–6070.
Murofushi T, Curthoys IS, Topple AN, Colebatch JG, Halmagyi GM: Responses of guinea pig primary vestibular neurons to clicks. Exp Brain Res 1995;103:174–178.
Murofushi T, Halmagyi GM, Yavor RA, Colebatch JG: Absent vestibular evoked myogenic potentials in vestibular neurolabyrinthitis. An indicator of inferior vestibular nerve involvement? Arch Otolaryngol Head Neck Surg 1996;122:845–848.
Murofushi T, Matsuzaki M, Mizuno M: Vestibular evoked myogenic potentials in patients with acoustic neuromas. Arch Otolaryngol Head Neck Surg 1998;124:509–512.
Murofushi T, Matsuzaki M, Wu CH: Short tone burst-evoked myogenic potentials on the sternocleidomastoid muscle: are these potentials also of vestibular origin? Arch Otolaryngol Head Neck Surg 1999;125:660–664.
Potter CN, Silverman LN: Characteristics of vestibular function and static balance skills in deaf children. Phys Ther 1984;64:1071–1075.
Rine RM, Cornwall G, Gan K, LoCascio C, O'Hare T, Robinson E, Rice M: Evidence of progressive delay of motor development in children with sensorineural hearing loss and concurrent vestibular dysfunction. Percept Mot Skills 2000;90:1101–1112.
Sennaroglu L, Saatci I: A new classification for cochleovestibular malformations. Laryngoscope 2002;112:2230–2241.
Sheykholeslami K, Megerian CA, Arnold JE, Kaga K: Vestibular-evoked myogenic potentials in infancy and early childhood. Laryngoscope 2005;115:1440–1444.
Shinjo Y, Jin Y, Kaga K: Assessment of vestibular function of infants and children with congenital and acquired deafness using the ice-water caloric test, rotational chair test and vestibular-evoked myogenic potential recording. Acta Otolaryngol 2007;127:736–747.
Suarez H, Angeli S, Suarez A, Rosales B, Carrera X, Alonso R: Balance sensory organization in children with profound hearing loss and cochlear implants. Int J Pediatr Otorhinolaryngol 2007;71:629–637.
Todt I, Hennies HC, Basta D, Ernst A: Vestibular dysfunction of patients with mutations of connexin 26. Neuroreport 2005;16:1179–1181.
Tribukait A, Brantberg K, Bergenius J: Function of semicircular canals, utricle and saccules in deaf children. Acta Otolaryngol 2004;124:41–48.
Tsukada K, Nishio S, Usami S, Deafness Gene Study Consortium: A large cohort study of *GJB2* mutations in Japanese hearing loss patients. Clin Genet 2010;78:464–470.
Viciana D, Lopez-Escamez JA: Short tone bursts are better than clicks for cervical vestibular-evoked myogenic potentials in clinical practice. Eur Arch Otorhinolaryngol 2012;269:1857–1863.
Wallacott MH, Assaiante C, Amblard B: Development of balance and gait control; in Bronstein AM, Brandt T, Wallacott MH, Nutt JG (eds): Clinical Disorders of Balance, Posture and Gait, ed 2. London, Arnold, 2004, pp 39–62.
Welgampola MS, Colebatch JG: Characteristics and clinical applications of vestibular-evoked myogenic potentials. Neurology 2005;64:1682–1688.
Zagólski O: Vestibular-evoked myogenic potentials and caloric stimulation in infants with congenital cytomegalovirus infection. J Laryngol Otol 2008;122:574–579.

Auris Nasus Larynx 40 (2013) 510–513

Contents lists available at SciVerse ScienceDirect

Auris Nasus Larynx

journal homepage: www.elsevier.com/locate/anl

Cochlear implantation in a patient with osteogenesis imperfecta

Yoshimi Makizumi, Akinori Kashio, Takashi Sakamoto, Shotaro Karino, Akinobu Kakigi, Shinichi Iwasaki, Tatsuya Yamasoba *

Department of Otolaryngology and Head and Neck Surgery, Graduate School of Medicine, The University of Tokyo, Japan

ARTICLE INFO

Article history:
Received 18 May 2012
Accepted 9 November 2012
Available online 6 December 2012

Keywords:
Cochlear implantation
Osteogenesis imperfecta
Facial nerve stimulation

ABSTRACT

Osteogenesis imperfecta (OI) is a connective tissue disorder characterized by a deficit in the synthesis of type I collagen. Hearing loss affects 42–58% of OI patients and progresses to deafness in 35–60% of these patients. For OI patients, cochlear implantation (CI) is the only promising treatment option. However, literature on CI in patients with OI is relatively rare. After CI, speech perception is generally good. However, among patients with severe demineralization of the cochlea, most patients are reported to have complications of facial nerve stimulation (FNS), preventing some patients from using the cochlear implant on a daily basis. Here we report a successful CI using a Nucleus CI24 Contour Advance cochlear implant in a patient with OI. Although high-resolution computed tomography (HRCT) showed extensive demineralization of the cochlea, intracochlear electrodes were inserted properly. The use of a modiolus-hugging device and the advance off-stylet technique contributed to the successful implantation, with no complications such as FNS or misplacement of electrodes. Therefore, CI can be used for treating deaf patients with OI.

1. Introduction

Osteogenesis imperfecta (OI) is a connective tissue disorder characterized by a deficit in the synthesis of type I collagen [1]. OI was first described by van der Hoeve and de Kleyn in 1917 [2] and, therefore, is also known as van der Hoeve–de Kleyn syndrome. The disease is characterized by brittle bones, blue sclerae, defective dentition and hearing loss [3]. Progressive hearing loss has been reported, including conductive, sensorineural, or mixed types [4]. Conductive hearing loss may be the result of a fracture or localized dehiscence of the stapedial arch, distal atrophy of the long process of the incus, or fixation of the stapedial footplate [1]. Sensorineural hearing loss is caused by microfractures, hemorrhage, and encroachment of reparative vascular and fibrous tissue in and around the cochlea [1]. Previous studies have reported hearing loss in 42–58% of OI patients and profound deafness in 35–60% of OI patients [5–9]. Hearing loss usually begins in the late teens in OI patients. The sensorineural component appears and progresses gradually in the third decade, resulting in profound deafness by the end of the fourth to fifth decade [7]. Cochlear implantation (CI) is the only treatment option for profound sensorineural hearing loss. However, the scientific and medical literature on CI in patients with OI is relatively rare [5–10]. After CI, speech perception is generally good. However, most patients with severe demineralization of the cochlea are reported to have complications of facial nerve stimulation (FNS). Several cases of electrode mis-insertion have also been reported. Some patients with such complications give up daily use of the cochlear implant [7,11].

Here, we report a successful CI using a Nucleus CI24 Contour Advance (CA) cochlear implant in a patient with OI. Although high-resolution computed tomography (HRCT) showed extensive demineralization of the cochlea, intracochlear electrodes were properly inserted without any of the common complications.

2. Case presentation

A female patient had several episodes of bone fractures due to minor trauma from childhood. At 18-years of age, she began to complain of bilateral hearing loss. A clinical examination revealed blue sclerae with hearing loss, and the patient was diagnosed as OI based on the clinical criteria [12] at the age of 21 years. The patient had no family history of OI or hearing loss, except for her grandfather who had presbycusis. At the age of 27 years, the patient underwent an ossiculoplasty of the left ear that unfortunately resulted in deafness. Subsequently, she began to wear a hearing aid in the right ear. At the age of 52 years, the patient consulted our department when her hearing acuity in the right ear worsened. An otoscopy examination revealed normal tympanic membranes in both ears. A pure-tone audiogram demonstrated

* Corresponding author at: Department of Otolaryngology and Head and Neck Surgery, Faculty of Medicine, The University of Tokyo, Hongo 7-3-1, Bunkyo-ku, Tokyo 113-8655, Japan. Tel.: +81 3 5800 8924; fax: +81 3 3814 9486.
E-mail address: tyamasoba-tky@umin.ac.jp (T. Yamasoba).

0385-8146/$ – see front matter © 2012 Elsevier Ireland Ltd. All rights reserved.
http://dx.doi.org/10.1016/j.anl.2012.10.006

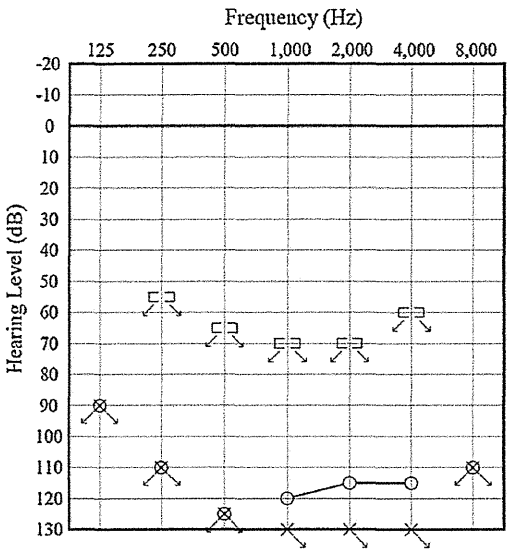

Fig. 1. Preoperative audiogram. A pure-tone audiogram demonstrated profound sensorineural hearing loss in both ears.

profound sensorineural hearing loss in both ears (Fig. 1). A speech discrimination test revealed no identification ability in both ears. Speech recognition scores with a hearing aid showed that only 10% of phonemes were recognized in the open set condition and 24% were recognized with verbal cues. The vestibular evoked myogenic potential (VEMP) was absent in both sides. A caloric test did not evoke nystagmus in either ear. A promontory stimulation test produced good auditory perception in both ears. HRCT revealed severe demineralization of the pericochlear and vestibular areas in both sides, and the outline of the cochlea was almost unrecognizable (Fig. 2). Magnetic resonance imaging (MRI) showed fluid intensity in the entire cavity of the right cochlea. However, fluid intensity in the scala tympani of the basal turn was decreased in the left cochlea (Fig. 3). The right and left cochlear nerves were well recognized on MRI.

Because there was a long period of auditory deprivation of the left ear and the MRI suggested partial occlusion in the basal turn, we decided to perform CI for the right ear. At the age of 54 years, the patient underwent surgery in the right ear to implant the Nucleus CI24R Contour Advance device. A mastoidectomy and a posterior tympanotomy were performed uneventfully. The foramen obturatum and the oval window were obliterated, and the round window was barely identified by the new bone formation of the promontory. We performed chocleostomy using the location of stapes as a landmark. The bone of the cochlear capsule was spongiotic and fragile; however, a cochleostomy was easily performed and the scala tympani was identified. All of the 22 electrodes were inserted successfully using the advanced off-stylet (AOS) technique. Postoperative neural response telemetry (NRT) showed good responses in all electrodes without FNS. Postoperative radiography and HRCT revealed the fully inserted electrodes inside the cochlea (Fig. 4). All of the electrodes showed normal impedance at first stimulation, and

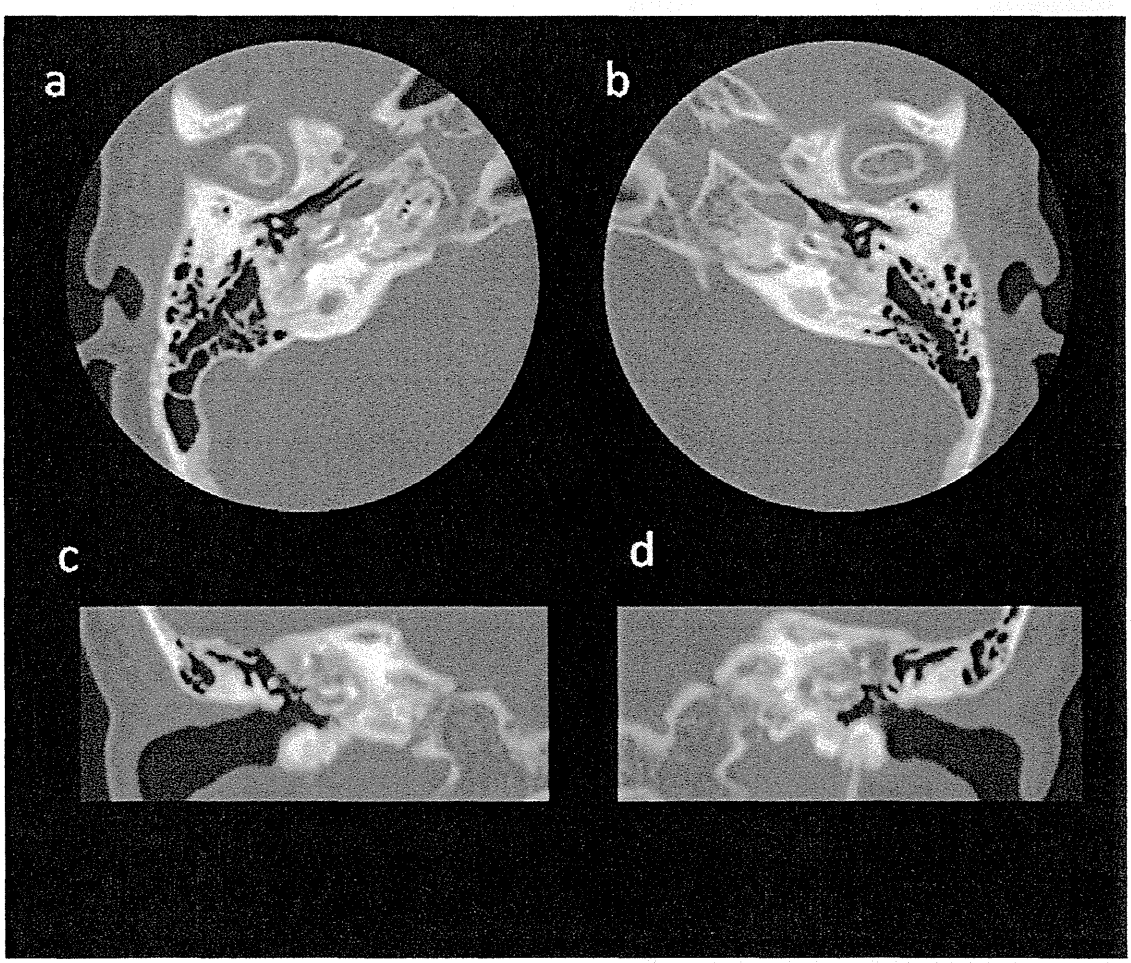

Fig. 2. Preoperative CT image of the cochlea. High resolution computed tomography (HRCT) revealed significant demineralization of the right and left pericochlear and vestibular areas, and the structures of the cochleae were almost unrecognizable.

Fig. 3. Preoperative MRI image of the cochlea. MRI demonstrated fluid content in the entire right cochlea. However, in the left cochlea, the fluid content in the scala tympani of the basal turn showed a defect, which suggested a partial occlusion.

no FNS was found during the stimulation. At the 6-month postoperative evaluation, the perception scores of monosyllables, words, and sentences using the CI and without any other cues were 62%, 70%, and 91%, respectively. These results indicated that the patient had good speech perception.

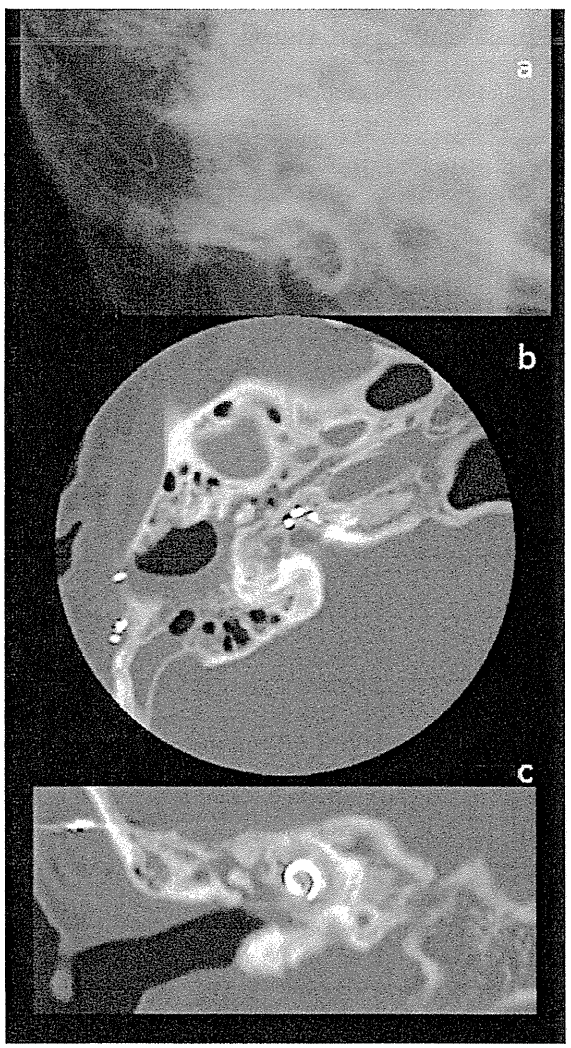

Fig. 4. Intraoperative radiograph and postoperative HRCT images of the cochlea. Intraoperative radiograph (a) and postoperative HRCT images (b and c) showed fully inserted electrodes.

3. Discussion

We have reported the case of an OI patient with a severely demineralized cochlea who underwent a successful operation for CI, resulting in good speech perception. No complications such as FNS and misplacement of electrodes were observed following the operation.

OI is a heterogeneous disease of the connective tissue caused by defective genes (*COL1A1* and *COL1A2*). *COL1A1* and *COL1A2* are responsible for the production of collagen type I, and mutations lead to defects in the bone matrix and connective tissue [7]. Recent studies have shown that reduced bone mineral density as a feature of OI and examining bone mineral density using the devices such as X-ray absorptiometry and peripheral quanitative computed tomography as well as genetic screening are becoming another powerful tool for the diagnosis of OI [13]. In this case, however, we made the diagnosis of OI based on the traditional criteria introduced by Sillence et al. [12]. Previous studies have reported various results for the prevalence of OI, ranging from 1/10,000 to 1/30,000 [6,14]. It has been reported that 2–35% of OI patients progress to deafness, with CI being the only promising treatment option [7–9]. To date, only 10 cases of CI with OI have been reported, including the present case. The HRCT findings of OI are as follows: (1) extensive dematerialized bone involving all or part of the otic capsule and extending as high as the upper margin of the superior semicircular canal; (2) fenestral manifestations caused by proliferation of bone, such as a narrow middle ear cavity, an enveloped stapes footplate, and obliterated windows with irregular and indistinct margins; and (3) involvement of the facial nerve canal in the dysplastic process [15]. These clear findings can lead surgeons to underestimate the remaining cochlear structure and space for electrodes thus improperly limiting the scope of CI. This may be the reason for the relatively small number of CIs reported for OI. In the present case, HRCT demonstrated extensive demineralization of the bony labyrinth, and the structure of cochlea was barely distinguishable. In contrast, a T2-weighted fast spin-echo (3D-FSE) MRI revealed a distinct fluid signal in the right cochlea. Based on this additional information provided by the MRI, we confidently decided to carry out CI.

In the present case, MRI showed a partial occlusion of the basal turn in the left ear. The previous ossiculoplasty might have elicited the occlusion, but we cannot deny the possibility that this occlusion was the result of ossification due to OI. Occlusion of the cochlea has also been reported in patients with otosclerosis, who have shown a similar proliferation of bones around the cochlea [16]. The genetic association with COL1A1 has been reported also in otosclerosis. Chen et al. suggested that otosclerosis has an association with single nucleotide polymorphisms in the regulatory regions of COL1A1, whereas OI is caused by a reduction in total COL1A1 mRNA secondary to mutations in COL1A1 [17]. It is possible that the association with COL1A1 in both of two diseases may cause the similar demineralization of the cochlea and that the difference in the mechanisms of COL1A1 disorder may determine the characteristics of each disease. As the present report shows, the condition of the cochlea should be carefully examined preoperatively by both HRCT and MRI. Otherwise, an evaluation by CT alone may lead to a misunderstanding of the operative indication for CI.

Because of severe demineralization of the otic capsule, CI in OI is challenging and is often accompanied by several complications. One such complication is FNS, and another is the misplacement of electrodes. Six patients with severe demineralization of the otic capsule have been reported to experience FNS as a complication after CI [5–8]. Most of the patients continued using the implant after switching off several

electrodes that caused the FNS. However, 2 patients discontinued use of the cochlear implant due to severe discomfort. It has been postulated that FNS is induced by deviant current spread throughout dehiscent or otospongiotic bone, where impedance is low, resulting in an electrical field in the proximity of the facial nerve [18]. Perimodiolar electrodes of the Nucleus CI24R CA device are tightly shielded against the lateral spread of current and theoretically are less likely to elicit FNS [19]. A CI study of patients with otosclerosis who had histopathologically similar demineralization of the cochlea showed a higher incidence (44%) of FNS in patients implanted with non modiolus-hugging devices than in those implanted with modiolus-hugging devices (10%) [20]. In the present case, no FNS occurred despite severe demineralization of the otic capsule. This is the first report of a successful CI with a perimodiolar designed electrode in an OI patient with severe demineralization of the cochlea. Additional cases are needed to establish the efficacy of the perimodiolar electrode for preventing FNS. However, perimodiolar designed electrodes may be preferable for OI patients to prevent FNS complications.

Another significant complication of CI in OI patients is misplacement of the electrodes. Two cases of misplacement have been reported. The risk of misplacement of the electrode array in a spongiotic otic capsule has also been described in patients with otosclerosis [20]. Cochlear otosclerosis is similar to OI because otospongiotic changes of the otic capsule and abnormal bone proliferation around a promontory of the otic capsule are observed in both conditions. In an OI patient, it is difficult to identify the round window niche or oval window [5]. Therefore, cochleostomy is challenging due to a lack of anatomical landmarks. Even when cochleostomy is performed in the proper place, the electrode can easily destroy the capsule and penetrate into the surrounding structures during insertion due to the soft and brittle nature of the cochlear bone. Recently, CI devices have been developed to minimize insertion trauma. The CA electrode may be used as an alternative to the traditional straight electrode, applying the AOS insertion technique so that the electrode does not touch the outer wall of the cochlea, thus reducing the risk of trauma to the cochlea [21]. With this technique, the slower insertion speed of the electrodes is also reported to impact the insertion force and reduce the risk of trauma [22]. Therefore, using this new, less traumatic device with a slower electrode insertion speed can prevent misplacement.

Our patient could recognize of 62% of phonemes, 70% of words, and 91% of sentences. Therefore, we concluded that the CI was successful. Berger et al. [23] reviewed the histopathology of the temporal bone in OI and suggested that progressive sensorineural hearing loss results from hemorrhage into the inner ear spaces. Subsequently, the accumulated cells and plasma proteins may disturb the inner ear dynamics and alter the electrolyte gradients. In this pathological condition, the spiral ganglion cells are assumed to be well preserved; therefore, good performance can be expected after CI. Nevertheless, 3 patients had an unsuccessful result in previous report. Two of these unsuccessful results were attributed to misplacement of the electrodes and severe FNS [7]. Another case involved a 6-year-old child who had profound sensorineural hearing loss from 6 months of age [8]. The poor result observed in this case can be attributed to the late age of implantation. These results show that if the electrodes are inserted properly within the appropriate period, sufficient speech perception can be expected and that CI surgery is a promising choice of treatment for OI.

4. Conclusion

We reported the case of an OI patient showing severe demineralization of the cochlea on HRCT. Preoperative MRI showed sufficient space for the CI in the basal turn of the right cochlea. All 22 intracochlear electrodes were successfully inserted, and no complications, such as FNS and mis-insertion, occurred. We attribute this success to the use of modiolus-hugging electrodes. The results of postoperative speech perception were good and consistent with those of previous reports.

Conflict of interest

None.

References

[1] Nager GT. Ostenogenesis imperfecta of the temporal bone and its relation to otosclerosis. Ann Otol Rhinol Laryngol 1988;97:585–93.
[2] van der Hoeve J, de Kleyn A. Blaue sclerae, knochenbruechigkeit und schwerhoerighkeit. Albrecht Von Graefes Arch Klin Exp Ophthalmol 1918;95:81–93.
[3] Proscop DJ, Kuivaniemi H, Tromp G. Hereditable disorders of connective tissue. In: Isselbacher E, Braunwald JD, Wilson JB, Martin AS, Fauci DL, Kasper, editors. Harrison's principles of internal medicine. 13th ed., McGraw-Hill International; 1994. p. 2111–3.
[4] Pedersen U. Hearing loss in patients with osteogenesis imperfecta. A clinical and audiological study of 201 patients. Scand Audiol 1984;13:67–74.
[5] Streubel SO, Lustig LR. Cochlear implantation in patients with osteogenesis imperfecta. Otolaryngol Head Neck Surg 2005;132:735–40.
[6] Cohen BJ. Osteogenesis imperfecta and hearing loss. Ear Nose Throat J 1984;63:283–8.
[7] Rotteveel LJ, Beynon AJ, Mens LH, Snik AF, Mulder JJ, Mylanus EA. Cochlear implantation in 3 patients with osteogenesis imperfecta: imaging, surgery and programming issues. Audiol Neurootol 2009;13:73–85.
[8] Migirov L, Henkin Y, Hildesheimer M, Kronenberg J. Cochlear implantation in a child with osteogenesis imperfecta. Int J Pediatr Otorhinolaryngol 2003;67:677–80.
[9] Huang TS, Yen PT, Liu SY. Cochlear implantation in a patient with osteogenesis imperfecta and otospongiosis. Am J Otolaryngol 1998;19:209–12.
[10] Szilvássy J, Jóri J, Czigner J, Tóth F, Szilvássy Z, Kiss JG. Cochlear implantation in osteogenesis imperfecta. Acta Otorhinolaryngol Belg 1998;52:253–6.
[11] Mens LH, Mulder JJ. Averaged electrode voltages in users of the Clarion cochlear implant device. Ann Otol Rhinol Laryngol 2002;111:370–5.
[12] Sillence DO, Senn A, Danks DM. Genetic heterogeneity in osteogenesis imperfecta. J Med Genet 1979;16:101–16.
[13] Swinnen FK, De Leenheer EM, Goemaere S, Cremers CW, Coucke PJ, Dhooge IJ. Association between bone mineral density and hearing loss in osteogenesis imperfecta. Laryngoscope 2012;122:401–8.
[14] Kuurila K, Grenman R, Johansson R, Kaitila I. Hearing loss in children with osteogenesis imperfecta. Eur J Pediatr 2000;159:515–9.
[15] Tabor EK, Curtin HD, Hirsch BE, May M. Osteogenesis inperfecta tarda: appearance of the temporal bones at CT. Radiology 1990;175:181–3.
[16] Ruckenstein MJ, Rafter KO, Montes M, Bigelow DC. Management of far advanced otosclerosis in the era of cochlear implantation. Otol Neurotol 2001;22:471–4.
[17] Chen W, Meyer NC, McKenna MJ, Pfister M, McBride Jr DJ, Fukushima K, et al. Single-nucleotide polymorphisms in the COL1A1 regulatory regions are associated with otosclerosis. Clin Genet 2007;71:406–14.
[18] Bigelow DC, Kay DJ, Rafter KO, Montes M, Knox GW, Yousem DM. Facial nerve stimulation from cochlear implants. Am J Otol 1998;19:163–9.
[19] Cohen LT, Richardson LM, Saunders E, Cowan RS. Spatial spread of neural excitation on cochlear implant recipients: comparison of improved ECAP method and psychophysical forward masking. Hear Res 2003;179:72–87.
[20] Rotteveel LJ, Proops DW, Ramsden RT, Saeed SR, van Olphen AF, Mylanus EA. Cochlear implantation in 53 patients with otosclerosis: demographics, computed tomographic scanning, surgery, and complications. Otol Neurotol 2004;25:943–52.
[21] Roland Jr JT. A model for cochlear implant electrode insertion and force evaluation: results with a new electrode design and insertion technique. Laryngoscope 2005;115:1325–39.
[22] Kontorinis G, Lenarz T, Stöver T, Paasche G. Impact of the insertion speed of cochlear implant electrodes on the insertion forces. Otol Neurotol 2011;32:565–70.
[23] Berger G, Hawke M, Johnson A, Proops D. Histopathology of the temporal bone in osteogenesis imperfecta congenita: a report of 5 cases. Laryngoscope 1985;95:193–9.

Original Paper

Audiology & Neurotology

Audiol Neurotol 2013;18:335–343
DOI: 10.1159/000354620

Received: March 11, 2013
Accepted after revision: July 22, 2013
Published online: October 2, 2013

Evaluation of the Internal Structure of Normal and Pathological Guinea Pig Cochleae Using Optical Coherence Tomography

Akinobu Kakigi[a] Yuya Takubo[b] Naoya Egami[a] Akinori Kashio[a]
Munetaka Ushio[a] Takashi Sakamoto[a] Shinji Yamashita[b] Tatsuya Yamasoba[a]

[a]Department of Otolaryngology, Faculty of Medicine, and [b]Research Center for Advanced Science and Technology, The University of Tokyo, Tokyo, Japan

Key Words
Cochlea · Optical coherence tomography · Endolymphatic hydrops · Strial atrophy · Organ of Corti

Abstract
Optical coherence tomography (OCT) makes it possible to visualize the internal structures of several organs, such as the eye, in vivo. Although visualization of the internal structures of the inner ear has been used to try and identify certain pathological conditions, attempts have failed mainly due to the thick bony capsule surrounding this end organ. After decalcifying the bony wall of the cochlea with ethylenediamine tetraacetic acid, we could clearly visualize its internal structures by using OCT. We identified endolymphatic hydrops, strial atrophy and damage to the organ of Corti, evident as a distention of Reissner's membrane, thinning of the lateral wall and flattening of the organ of Corti, respectively. When specimens embedded in paraffin, sliced and stained with hematoxylin and eosin (HE) were examined under a light microscope, the OCT images of normal and pathological cochleae were virtually identical with those of the HE specimens, except that the HE specimens exhibited several artifacts unrecognized in OCT images, which were considered to be induced during the preparation process. Since OCT enables one to obtain arbitrary plane images by manipulating the slice axis of the specimens and avoids any misinterpretation due to artifacts induced during histological preparation, our technique would be useful for examining cochlear pathologies without or prior to histological evaluations.

Introduction

Structural integrity of the cochlea is required to maintain normal auditory function. Certain types of cochlear pathologies have been known to be closely associated with impaired auditory function. Since the cochlea is housed deeply within the temporal bone, however, it is extremely difficult to examine its structure in vivo. Structural observation has primarily been limited to histological methods, which require several procedures such as chemical fixation, dissection of the tissues, embedment in a mold such as paraffin, and sectioning. These procedures can introduce significant changes in tissue integrity and organization [Slepecky and Ulfendahl, 1988; Brunschwig and Salt, 1997], limiting the generality and overall value of results. To better visualize the internal structure of the cochlea, an emerging noninvasive imaging modality, optical coherence tomography (OCT), has been applied.

KARGER

1420–3030/13/0185–0335$38.00/0

E-Mail karger@karger.com
www.karger.com/aud

Akinobu Kakigi
Department of Otolaryngology, Faculty of Medicine, University of Tokyo
7-3-1 Hongo, Bunkyo-ku
Tokyo 113-8655 (Japan)
E-Mail kakigi-tky@umin.ac.jp

OCT uses low-coherence interferometry to produce a two-dimensional image of internal tissue microstructures [Huang et al., 1991]. It uses light to discern intrinsic differences in tissue structure and uses coherence gating to localize the origin of the reflected optic signal. Internal tissue microstructures can be visualized with axial and lateral spatial resolutions in the order of 10 μm and a depth of penetration of approximately 2–3 mm depending on tissue translucency. This technology has become widely established for clinical applications in the fields of ophthalmology and dermatology to visualize the translucent tissues of the eye [Izatt et al., 1994] and superficial tissues of the skin [Welzel, 2001].

Clinical use of OCT has since been extended to the fields of cardiology and gastroenterology in visualizing deeper structures such as coronary vessels [Jang et al., 2002] and the gastrointestinal tract [Shen and Zuccaro, 2004]. Most recently, OCT has been used in the field of otolaryngology to visualize the larynx [Wong et al., 2005]. However, clinical use of OCT has been limited in other organs including the inner ear because of its relatively limited depth of penetration and the turbidity of most biological tissues. In fact, previous studies allowed visualization of only limited areas of the cochleae [Wong et al., 2004; Lin et al., 2008; Sepehr et al., 2008; Subhash et al., 2010]. For example, Sepehr et al. [2008] drilled the otic capsule of pigs obtained within 1 h of sacrifice and found that in the areas of thinned bone, acceptable images were obtained of the spiral ligament, stria vascularis, Reissner's membrane, basilar membrane, tectorial membrane, scala media, scala tympani and scala vestibuli; however, the bone was too thick for adequate light penetration in the areas where it was not thinned.

Subhash et al. [2010] obtained in vivo OCT images of a portion of the apical, middle and basal turns of the mouse cochlea through a surgically prepared opening via the bone of the bulla. They demonstrated that spectral-domain OCT could be used for in vivo imaging of important morphological features within the mouse cochlea, such as the otic capsule and structures within, including Reissner's membrane, the basilar membrane, the tectorial membrane, the organ of Corti and the modiolus of the apical and middle turns, but the resolution and quality were unsatisfactory.

In the current study, we observed the cochleae by OCT after decalcification of the otic bony capsule. We could clearly visualize normal internal structures of the cochleae and identify endolymphatic hydrops (EH), strial atrophy and damage to the organ of Corti, which appeared as a distention of Reissner's membrane, thinning of the lateral wall and flattening of the organ of Corti, respectively. This technology can prevent the misinterpretation of histological findings due to artifacts induced during histological preparation and thus is of great value in investigating the internal structural change of various types of cochlear damage.

Materials and Methods

Animals

A total of 20 Hartley guinea pigs with a positive Preyer reflex and weighing approximately 300 g were used. They were allocated to the following four groups, each consisting of 5 animals: (1) normal control group (no surgical procedure or treatment); (2) EH group (electrocauterization of the endolymphatic sac (ES), and a 4-week feeding); (3) kanamycin sulfate-ethacrynic acid (KM-EA) group (no surgical procedures, but intravenous administration of KM and EA and a 2-day feeding); and (4) streptomycin sulfate (SM) group (perilymphatic perfusion with 20% SM and a 4-month feeding). These experiments were approved by the Tokyo University animal care and use committee, and conformed to the Animal Welfare Act and the guiding principles for animal care produced by the Ministry of Education, Culture, Sports and Technology, Japan.

Surgical Procedure for the Electrocauterization of ES

EH can be either primary or secondary. Primary idiopathic EH (known as Ménière's disease) occurs for no known reason, while secondary EH appears to occur in response to an event or underlying condition (e.g. following head trauma or ear surgery, or with other inner ear disorders, allergies or systemic disorders such autoimmune disorders). EH was initially reported in patients with Ménière's disease independently by Yamakawa [1938] and Hallpike and Cairns [1938] and has since been found to be frequent in patients with Ménière's disease. EH represents a histopathological finding in which the structures bounding the endolymphatic space are distended by an enlargement of endolymphatic volume. The most widely studied animal model of EH was created by surgical ablation of the endolymphatic duct and sac in guinea pigs [Kimura and Schuknecht, 1965; Kimura, 1967].

To induce EH, we performed electrocauterization of the ES. Animals were anesthetized with an intraperitoneal injection of ketamine (35 mg/kg) and xylazine (5 mg/kg) and received local anesthesia with Xylocaine in sterile conditions. Then, they were placed in a prone position with a head holder and underwent a dorsal midline scalp incision under a Carl Zeiss operation microscope. The left occipital bone was removed to visually expose the ES via an epidural occipital approach. Then, the extraosseous portion of the sac was cauterized electrically so as not to injure the sigmoid sinus with the bipolar electrocoagulator (Surgitron Model FFPF; Ellman International Inc., Hewlett, N.Y., USA). The skin incision was sutured and the animals were allowed to survive for 4 weeks.

Procedures for Intravenous Administration of KM and EA

Auditory hair cells can be damaged and lost as a consequence of acoustic trauma, treatment with ototoxic agents, infections, autoimmune pathologies and genetic susceptibilities or as a part of the aging process. The loss of auditory hair cells in the human cochlea is a leading cause of permanent hearing deficits, currently affecting an estimated 600 million worldwide. In recent studies, loop diuret-

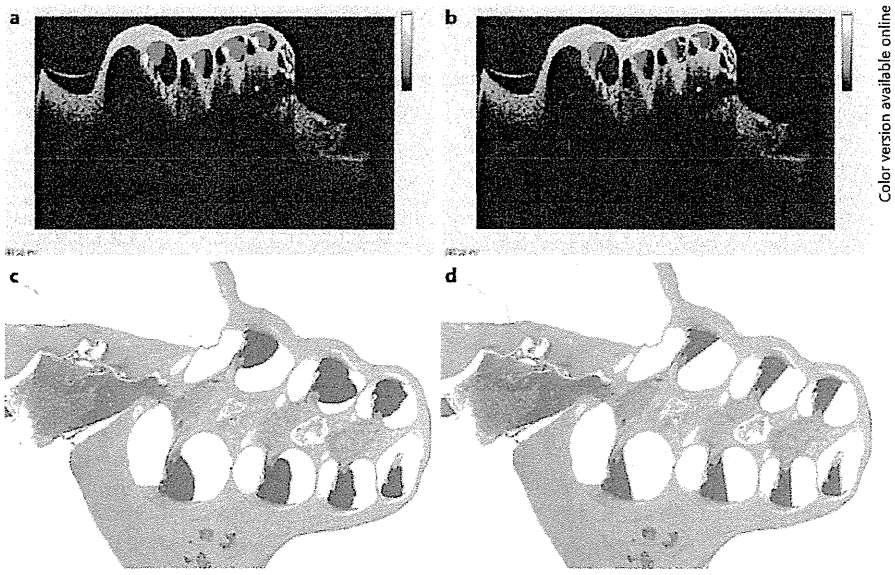

Fig. 1. Parameters for quantitative assessment of changes in endolymphatic space, organ of Corti and lateral wall. **a** Cross-sectional area of the dilated scala media (red areas), organ of Corti (yellow areas) and upper part of the lateral wall over the extended line of the lower level of the basilar membrane (green area) in an OCT image. **b** Cross-sectional area of the original scala media (blue areas) enclosed by a straight line segment. This line segment represents the position of the idealized Reissner's membrane at the upper margin of the stria vascularis to its normal medial attachment at the spiral limbus. **c** Cross-sectional area of the dilated scala media (red areas) of an HE specimen. **d** Cross-sectional area of the original scala media (blue areas) of an HE specimen. Colors refer to the online version only.

ics have been used to augment the ototoxic effect of aminoglycoside antibiotics and eliminate hair cells in mammals [Xu et al., 1993; Yamasoba and Kondo, 2006; Kashio et al., 2007; Taylor et al., 2008].

To induce degeneration of the organ of Corti, animals were given KM (Meiji, Tokyo, Japan) and EA (Sigma-Aldrich). They were anesthetized with an intraperitoneal injection of ketamine (35 mg/kg) and xylazine (5 mg/kg). A single dose of KM (400 mg/kg) was injected subcutaneously; 2 h after the KM injection, EA (50 mg/kg) was infused into the jugular vein as previously described [Yamasoba and Kondo, 2006]. The animals were then allowed to survive for 2 days after deafening.

Procedures for Perilymphatic Perfusion with 20% SM

Strial atrophy is one of the leading causes of deafness and three major etiologic factors have been reported: hereditary strial hypoplasia/atrophy [Gates et al., 1999; Ohlemiller et al., 2006], aging [Schuknecht and Gacek, 1993] and ototoxicity due to loop diuretics or the erythromycin group of antibiotics [Arnold et al., 1981; McGhan and Merchant, 2003].

To induce both hair cell loss and strial atrophy, animals underwent perilymphatic perfusion with 20% SM (Meiji) dissolved in Ringer's solution (Fuso, Osaka, Japan). The animals were anesthetized with an intraperitoneal injection of ketamine (35 mg/kg) and xylazine (5 mg/kg). The left cochlea was exposed using the lateral approach, and both the scala tympani and the scala vestibuli of four cochlear turns were perfused as follows. A 20% SM solution was gently perfused into the scala tympani through the round window membrane until the solution flowed out from the drilled hole adjacent to the oval window, as previously described [Terayama et al., 1977]. After the perfusion, the tympanic cavity was cleaned, the skin incision closed and the animals allowed to survive for 4 weeks.

OCT and Histological Observations

To observe the cochleae by OCT, all animals were given physiological saline from the left ventricle under deep anesthesia with ketamine and xylazine and fixed with 10% formalin. Both temporal bones were obtained immediately following the fixation and kept in a 10% formalin solution for 1 week. Subsequently, the specimens underwent decalcification in ethylenediamine tetraacetic acid (EDTA) for 14 days. Then we obtained midmodiolar images of the cochleae by using the Santec OCT system controlled by Inner Vision (Santec Co., Aichi, Japan). The characteristics of the Santec OCT system were as follows. The center wavelength band was 1,320 nm and the band width 90 nm. The axial and lateral resolutions were 12.0 and 17.0 μm, respectively. The measurement speed and frame rate were 50,000 lines/scan and 100 frames/s, respectively. The image depth and width were 6.0 and 10.0 mm, respectively. After OCT images were obtained, the temporal bones were dehydrated in increasingly higher concentrations of alcohol, embedded in paraffin and cut serially at 6 μm in the plane parallel to the modiolus to obtain approximately the same plane as the OCT image. The sections were stained with hematoxylin and eosin (HE) and observed under a light microscope [light microscopic mode of the BZ-9000 fluorescence microscope (Keyence, Osaka, Japan) controlled by BZ-II Analyzer (Keyence) software].

Quantitative Assessment of Endolymphatic Space, Organ of Corti and Lateral Wall

We used the digital image measurement software Micro Analyzer version 1.1 (Nippon Poladigital Co. Ltd, Tokyo, Japan) for quantitative assessment. In the EH group, we compared the degree of EH between OCT and HE images. For the quantitative assessment of endolymphatic space variations of the cochlea, we measured the increase in the cross-sectional area of the scala media (IR-S) over that in the midmodiolar sections. For this analysis, we used the following two parameters in the basal, second, third and apical turns, not including the hook portion: (1) the cross-sectional area of the dilated scala media (fig. 1a, c; red areas) and (2) the cross-sectional area of the original scala media (fig. 1b, d; blue areas) which were enclosed by a straight line segment. This line segment represents the position of the idealized Reissner's membrane at the upper margin

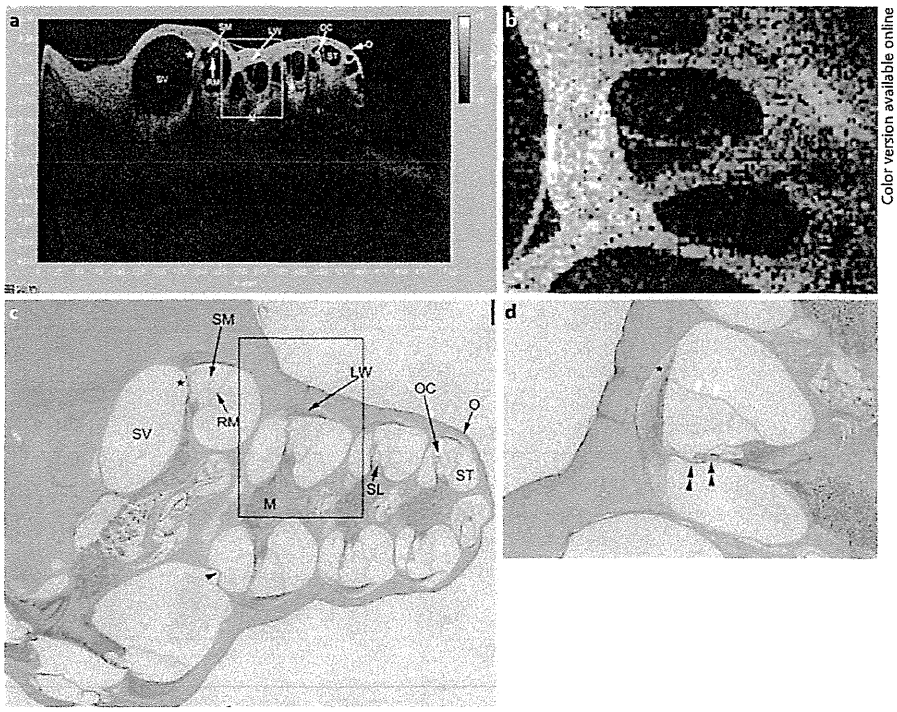

Fig. 2. a Representative cross-sectional OCT image of all turns of the spiral-shaped cochlea. **b** Magnified image (turned 90°) of the rectangular area in **a**. **c** Cross-sectional image of an HE specimen, using a light microscope. HE specimens exhibited several artifacts such as bending of the interscalar septum and basilar membrane and folding of Reissner's membrane as a consequence of separating the spiral ligament from the bony wall. The proportion of the area of the organ of Corti is smaller in the HE specimen (star) than in the OCT image (**a**; white star), especially in the basal turn. **d** Magnified image of the rectangular area in **c**. O = Otic capsule; M = modiolus; RM = Reissner's membrane; OC = organ of Corti; SL = spiral limbus; LW = lateral wall consisting of stria vascularis and spiral ligament; ST = scala tympani; SM = scala media; SV = scala vestibuli; arrowhead = bending of interscalar septum; double arrowheads = bending of basilar membrane; white arrowheads = folding of Reissner's membrane; asterisk = separating spiral ligament from bony wall.

of the stria vascularis to its normal medial attachment at the spiral limbus. From these parameters, we calculated the increase (%) in IR-S in the four turns with the following formula:

Total IR-S (%) = 100 × (red area – blue area)/blue area

Statistical Analysis

Data are presented as means ± SD, and they were compared by the paired Student t test. Differences were regarded as significant when $p < 0.05$.

We compared the degree of flattening of the organ of Corti and strial atrophy between the normal control and KM-EA groups and between the normal control and SM groups, respectively. To analyze the flattening of the organ of Corti, we used the following parameter in the basal, second, third and apical turns, not including the hook portion: the cross-sectional area of the organ of Corti (fig. 1a; yellow areas). Data for each turn were separately compared by Student's t test, and a difference was regarded as significant when $p < 0.05$. For the analysis of strial atrophy, we used the following parameter in the second turn: the cross-sectional area of the upper part of the lateral wall over the extended line of the lower level of the basilar membrane (fig. 1a; green area). We selected the second turn for the assessment because there was no proliferative change such as fibrosis.

Results

Normal Control Group

OCT provided detailed internal structures of the normal cochleae. We clearly identified not only the otic capsule and the modiolus, but also Reissner's membrane, the organ of Corti, the spiral limbus, the lateral wall consisting of the stria vascularis and spiral ligament in all four turns of the midmodiolar section (fig. 2a, b). The scalae tympani, media and vestibuli were clearly distinguishable. The OCT images were virtually identical with the corresponding histological sections (fig. 2c, d), although the HE specimens exhibited several artifacts such as the bending of the interscalar septum and basilar membrane and the folding of Reissner's membrane as a consequence of the separation of the spiral ligament from the bony wall. Concerning the organ of Corti, the proportion of the area was smaller in the HE specimen than in the OCT image, especially in the basal turn.

EH Group

OCT clearly demonstrated the presence of EH in all 5 cases 4 weeks after electrocauterization of the ES. In a case shown in figure 3a, mild but distinct hydrops was observed in the basal and second turns, and the hydrops was most evident in the third turn (fig. 3b, d). The spiral ligament, stria vascularis and organ of Corti appeared normal. A midmodiolar HE-stained section in this ear showed similar histological findings (fig. 3c), although the extent of EH was greater in the histological specimens

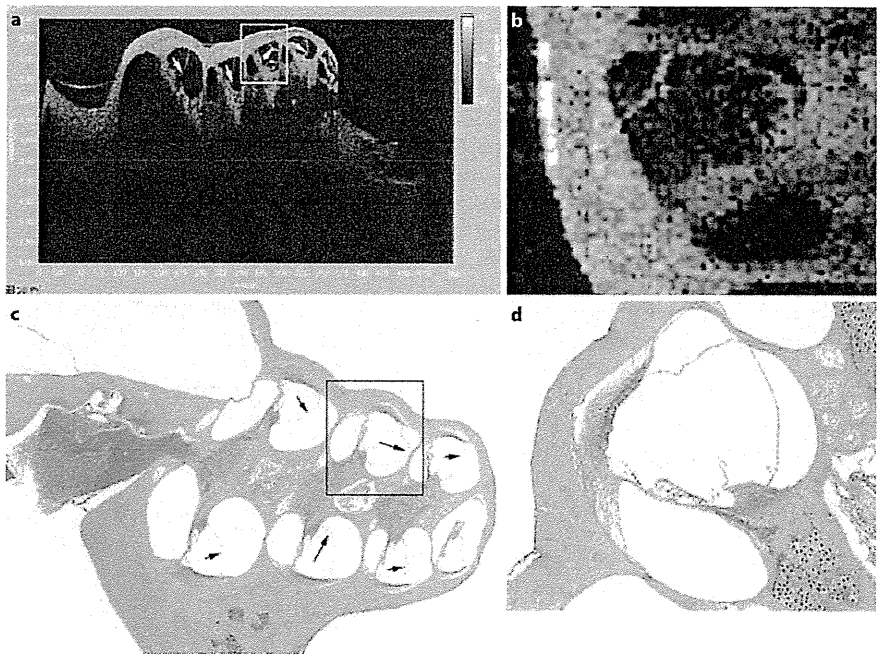

Fig. 3. **a** Representative cross-sectional OCT image of the cochlea in animals with electrocauterization of the ES. Mild but distinct hydrops was found in the basal and second turns, and hydrops was most evident in the third turn. **b** Magnified image of the rectangular area in **a**. **c** Cross-sectional image of an HE specimen, using a light microscope. A midmodiolar HE-stained section in this ear showed similar histological findings, although the extent of EH was greater in the histological specimens than in the OCT images. There are several artifacts similar to those seen in the normal cochlea. Note that hydrops was most evident in this turn. **d** Magnified image of the rectangular area in **c**. Arrows = Distention of Reissner's membrane.

than in the OCT images (fig. 4). Further, there were several artifacts similar to those seen in the normal cochlea. Figure 4 shows the IR-S in OCT and HE images: 54.3 ± 4.05% and 62.4 ± 6.51%, respectively. The IR-S was statistically larger in the HE than in the OCT images (paired Student's t test, $p < 0.05$).

KM-EA Group

Two days after the treatment with KM and EA, all animals lost the Preyer reflex and exhibited degeneration of the organ of Corti in all turns (fig. 5a). In a case shown in figure 5b, the flattening of the organ of Corti was obvious in the third and apical turns, whereas the spiral ligament and stria vascularis appeared normal. A slight collapse of Reissner's membrane was seen in all four turns. A midmodiolar HE-stained section in this ear showed similar histological findings, except that there was no collapse of Reissner's membrane (fig. 5e, f). The difference regarding Reissner's membrane between the OCT and histological findings may have been caused by histological preparation. Further, there were several artifacts similar to those seen in the normal cochlea. To assess the effects of KM-EA treatment on the organ of Corti, a comparison of the normalized size ratio of the organ of Corti (size of the targeted organ of Corti/average of the size of the normal organ of Corti) was made between the normal control and KM-EK groups, using OCT images. The normalized size

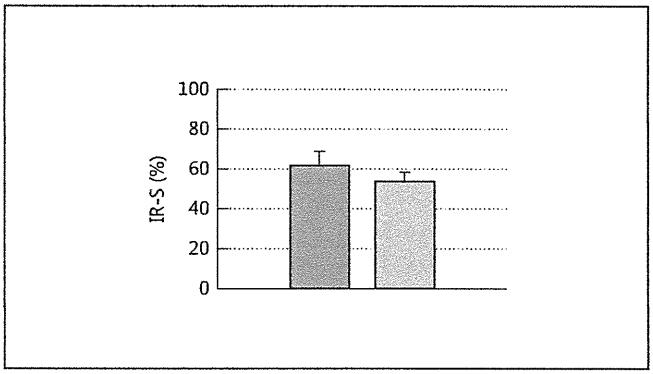

Fig. 4. Comparison of IR-S between OCT (light gray) and HE (dark gray) images. The IR-S (means ± SD) on the OCT and HE images were 54.3 ± 4.05% (n = 5) and 62.4 ± 6.51% (n = 5), respectively. The IR-S on the HE images was statistically larger than that on the OCT images (paired Student's t test, $p < 0.05$).

ratios of the basal, second, third and apical turns were 0.63 ± 0.14, 0.78 ± 0.16, 0.51 ± 0.10 and 0.58 ± 0.14, respectively, in the KM-EA group (n = 5; fig. 6). The KM-EA treatment resulted in a marked decrease in normalized size ratio of the organ of Corti. The decreases in the basal, second, third and apical turns were significant at $p < 0.001$, $p < 0.05$, $p < 0.001$ and $p < 0.05$, respectively (Student's t test).

Fig. 5. **a** Representative cross-sectional OCT image of the cochlea in animals with intravenous administration of KM and EA. The flattening of the organ of Corti was obvious in the third and apical turns. The spiral ligament and stria vascularis appeared normal. A slight collapse of Reissner's membrane was seen in all four turns. **b** Magnified image of the rectangular area in **a**. **c** Representative cross-sectional OCT image of the cochlea in the normal group. **d** Magnified image of the rectangular area in **c**. **e** A midmodiolar HE-stained section showed similar histological findings, although there was no collapse of Reissner's membrane. There are several artifacts similar to those seen in the normal cochlea. Note that flattening of the organ of Corti was evident. **f** Magnified image of the rectangular area in **e**. Arrows = Flattening of the organ of Corti.

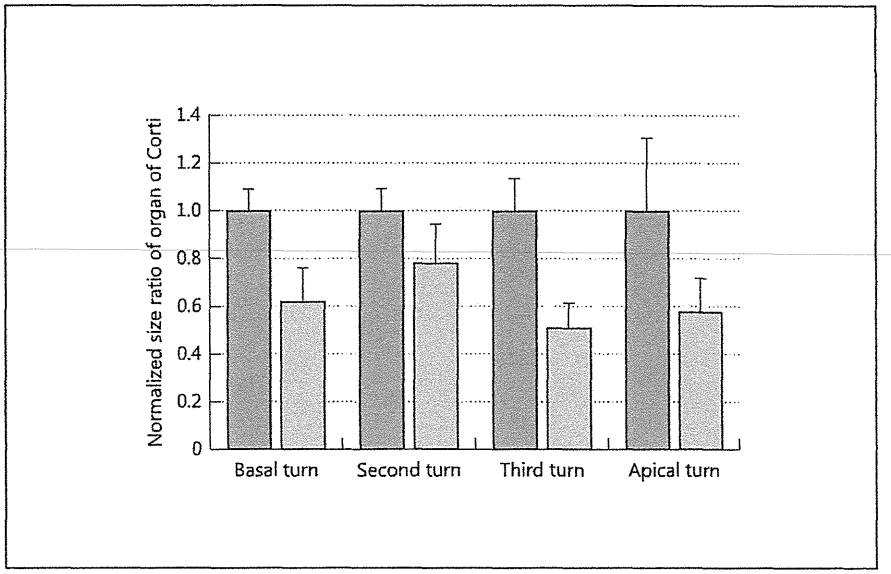

Fig. 6. Comparison of normalized size ratio (size of organ of Corti/averaged size of normal organ of Corti) of organ of Corti between normal control (dark gray) and KM-EA (light gray) groups, using OCT images. The normalized size ratios (means ± SD) of the basal, second, third and apical turns were 1.00 ± 0.09, 1.00 ± 0.09, 1.00 ± 0.14 and 1.00 ± 0.31, respectively, in the normal control group (n = 5), and 0.63 ± 0.14, 0.78 ± 0.16, 0.51 ± 0.10 and 0.58 ± 0.14, respectively, in the KM-EA group (n = 5). The decreases in the basal, second, third and apical turns were significant at $p < 0.001$, $p < 0.05$, $p < 0.001$ and $p < 0.05$, respectively (Student's t test).

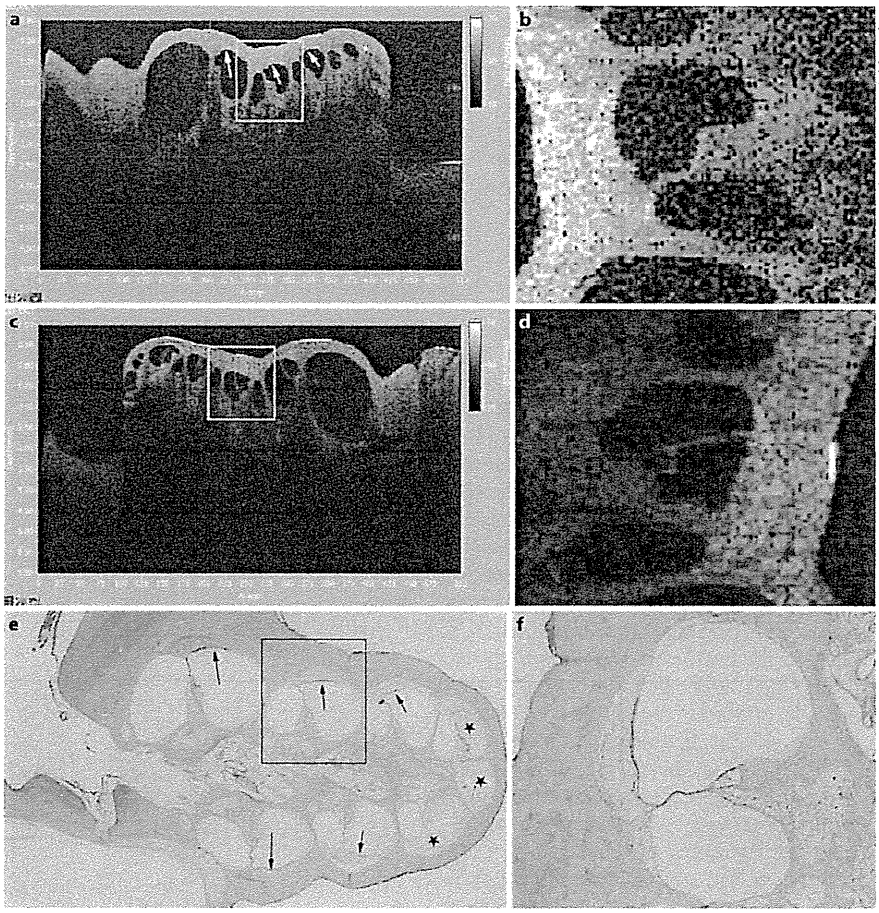

Fig. 7. **a** Representative cross-sectional OCT image of the cochlea in animals with perilymphatic perfusion with SM. Strial atrophy and flattening of the organ of Corti were seen in the basal, second and third turns. The strial atrophy reflected that the curvature of the medial surface increased in the lateral wall. A remarkable collapse of Reissner's membrane was also seen. In the apical turn, the fibrosis of the organ was remarkable. **b** Magnified image of the rectangular area in **a**. **c** Representative cross-sectional OCT image of the cochlea in the control ear. **d** Magnified image of the rectangular area in **c**. **e** Optical cross-sectional image of an HE specimen, using a light microscope. There are the same artifacts in the HE specimen as seen in the normal cochlea. **f** Magnified image of the rectangular area in **e**. Arrows = Strial atrophy; stars = fibrosis.

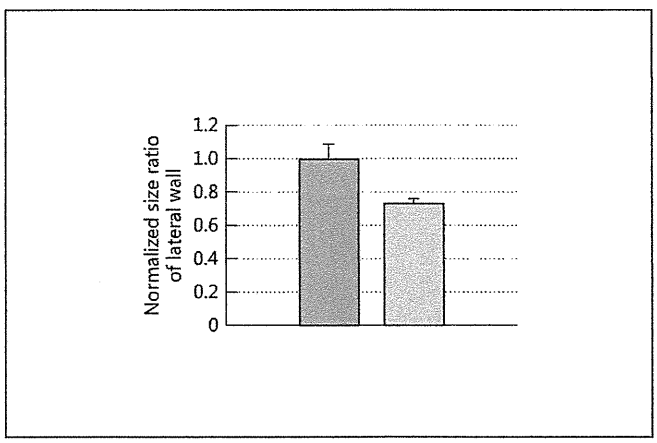

Fig. 8. Comparison of normalized size ratio (size of lateral wall/averaged size of normal lateral wall) of lateral wall between normal control (dark gray) and SM (light gray) groups, using OCT images. The normalized size ratio (mean ± SD) of the second turn was 1.00 ± 0.08 in the normal control group (n = 5) and 0.74 ± 0.02 in the SM group (n = 5). The decrease in the second turn was significant at $p < 0.001$ (Student's t test).

SM Group

The strial atrophy and damage to the organ of Corti were evident in all cases 4 weeks after perilymphatic perfusion with 20% SM (fig. 7a, b). Strial atrophy and flattening of the organ of Corti were seen mostly in the basal, second and third turns. The strial atrophy reflected that the curvature of the medial surface increased in the lateral wall. The remarkable collapse of Reissner's membrane was also seen mostly in the basal, second and third turns. In some animals, fibrosis was observed in the apical part of the cochlea. The OCT images were comparable with the corresponding histological sections (fig. 7e, f), although the loss of spiral ganglion cells observed in the HE specimen could not be visualized by OCT because of the limited spatial resolution and depth of penetration. To assess the effects of SM treatment on the lateral wall, a comparison of the normalized size ratio of the lateral wall was made between the normal control and SM groups, using OCT images. The normalized size ratio of the second turn was 0.74 ± 0.02 in the SM group (n = 5;